Proceedings IRF2020: 7th International Conference Integrity-Reliability-Failure.
J.F. Silva Gomes and S.A. Meguid (editors), INEGI-FEUP (2020), pp.965-970.
https://paginas.fe.up.pt/~irf/Proceedings_IRF2020/

PAPER REF: 17305

SYNCHRONIZATION IN REAL TIME OF TWO STEWART PLATFORMS

Josep M. Rossell[1(*)], Jesús Vicente-Rodrigo[2], Víctor Barcons[2]
[1]Department of Mathematics, Universitat Politècnica de Catalunya (UPC), Manresa, Barcelona, Spain
[2]EMIT, Universitat Politècnica de Catalunya (UPC), Manresa, Barcelona, Spain
[(*)]*Email:* josep.maria.rossell@upc.edu

ABSTRACT

This paper presents two mechanisms that have been designed, built and put into operation by our research team at the Universitat Politècnica de Catalunya (UPC), Barcelona (Spain) which have many practical applications in the scientific, industrial and academic fields: the Stewart platforms. They are electromechanical systems capable of moving with six degrees of freedom, that is, three translations and three rotations that allow simulating the movement of any object in the space. The characteristics of a Stewart platform for its design, assembly and construction are presented. However, the main contribution of this paper is to demonstrate that it is possible to synchronize, in real time, both platforms when one of them is randomly moving and the other follows with high precision the movements of the first platform. The details about the algorithms and synchronization method are provided.

Keywords: Stewart platforms, parallel robots, synchronization, real-time control.

INTRODUCTION

A Stewart platform is considered as a complex mechatronic system due to different topics involved in it: mechanics, electronics, computing and control. This type of robot is a six degree-of-freedom manipulator mechanism composed by two parallel platforms, a base platform and a top plate, connected by six telescopic and extensible legs. In order to change the position of the top plate relative to the bottom plate, the legs must move in coordination to achieve a desired displacement.

The first Stewart platform was designed as a flight simulator in 1965 [1], but recently it has been used in industry areas such as energy generation, automotive, mechanics, civil engineering or aeronautics. Some applications can be found in machine tool technology [2], precision laser cutting [3], precision surgery [4], positioning systems for radio telescopes [5] or vehicle suspensions [6]. In addition, other potential applications are on ships, buoys or floating platforms at sea supporting devices such as precision instrumentation systems or cranes.

For real-time operation it is crucial to select efficient methods avoiding time-consuming computation. LabVIEW has been chosen as the software to perform the movements and control of the platforms, a graphical programming environmental for developing flexible and scalable applications.

Although certain companies construct some models of Stewart platforms, it should be noted that their cost is very high and, in addition, they usually work with their own software that does not allow modifications to be introduced to what is programmed by the manufacturer. For this reason, our research team has designed and built two Stewart platforms of different sizes but with similar characteristics, in order to perform many experimental simulations (see Figure 1).

Fig. 1 - Two Stewart platforms designed and constructed by our research team of the UPC

DESIGN OF A STEWART PLATFORM

Let us denote $O = [O; 0,0,0]$ the origin of the base, by $B = [O; x, y, z]$ the reference system of the platform base and by $P = [O'; x', y', z']$ the reference system of the top plate. Let b_i and p_i, $i = 1, \dots, 6$, the anchor points of the actuators in the base and the top plate, respectively (see Figure 2). The angles among the anchor points are computed in the following form:

$$\alpha_i = \frac{\pi}{3} i - \frac{\theta_B}{2}, \text{ for } i = 1,3,5 \quad \text{and} \quad \alpha_i = \alpha_{i-1} + \theta_B, \text{ for } i = 2,4,6 \tag{1}$$

$$\beta_i = \frac{\pi}{3} i - \frac{\theta_P}{2}, \text{ for } i = 1,3,5 \quad \text{and} \quad \beta_i = \beta_{i-1} + \theta_P, \text{ for } i = 2,4,6 \tag{2}$$

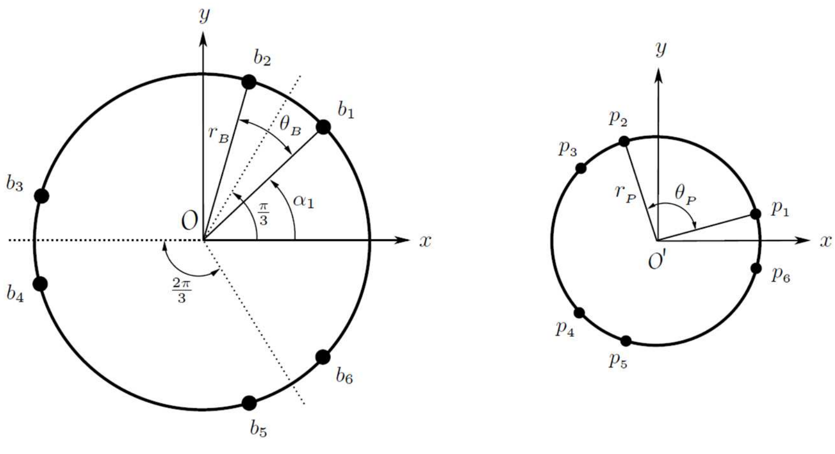

Fig. 2 - Anchor points at the base and the top plate of a Stewart platform

The location points b_i are described by the vectors $b_i = [r_B \cos \alpha_i, \; r_B \sin \alpha_i, \; 0\,]^T$, where r_B is the radius of the base and p_i by the vectors $p_i = [r_P \cos \beta_i, \; r_P \sin \beta, \; 0\,]^T$, where r_P is the radius of the top plate.

INVERSE KINEMATICS APPROACH

Obviously, a Stewart platform has a nonlinear character due to the Euler rotation matrices and consequently kinematic constraints appear. This is the reason why we cannot use forward kinematics methodology because it requires the solution of many nonlinear equations, mainly when a real-time control is needed. Furthermore, the forward kinematic problem has, in general, more than one solution.

Once the platform is mechanically configured, the methodology used for the movement and control will be the inverse kinematics (see Figure 3). It consists in computing the length that each actuator must have, that is, $L(t) = [l_1(t), \dots, l_6(t)]^T$, from the position and inclination of the upper disc, at each instant of time t.

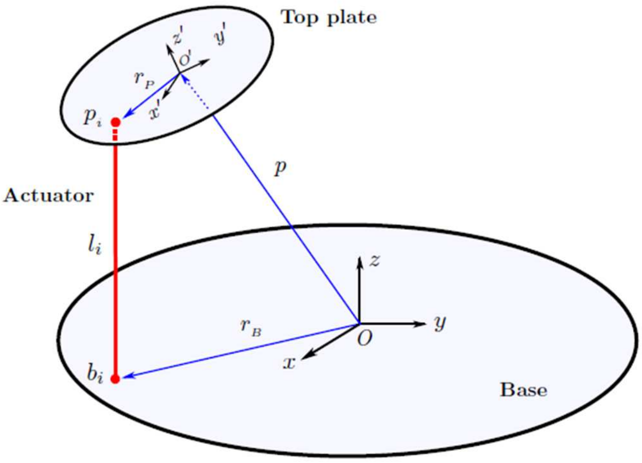

Fig. 3 - Inverse kinematic scheme of a Stewart platform

For any position of O' and orientation of the top plate, at any time t, there exists a unique position of the legs providing such position and orientation. Thus, we can compute

$$L_i(t) = \|p(t) + R(t)\, p_i - b_i\|, \quad \text{for } i = 1, \dots 6, \tag{3}$$

where $L_i(t)$ is the desired length of the leg *i*, at instant t, according to a prescribed motion, and p_i, b_i, for $i = 1, \dots 6$, are the attachment points given previously. The matrix R=R(t) is an orthogonal rotation matrix (Euler matrix) that specifies the orientation of the top plate with respect to the base. It depends on the choice of rotation axis sequence. In this paper we consider the following matrix R:

$$R = R_z(\alpha)R_y(\beta)R_x(\gamma) = \begin{bmatrix} r_{11} & r_{12} & r_{13} \\ r_{21} & r_{22} & r_{23} \\ r_{31} & r_{32} & r_{33} \end{bmatrix} \tag{4}$$

with

$$R_x(\gamma) = \begin{bmatrix} 1 & 0 & 0 \\ 0 & c_\gamma & -s_\gamma \\ 0 & s_\gamma & c_\gamma \end{bmatrix}, \quad R_y(\beta) = \begin{bmatrix} c_\beta & 0 & s_\beta \\ 0 & 1 & 0 \\ -s_\beta & 0 & c_\beta \end{bmatrix}, \quad R_z(\alpha) = \begin{bmatrix} c_\alpha & -s_\alpha & 0 \\ s_\alpha & c_\alpha & 0 \\ 0 & 0 & 1 \end{bmatrix}, \tag{5}$$

where

$$s_\alpha = \sin\alpha, \quad s_\beta = \sin\beta, \quad s_\gamma = \sin\gamma, \quad c_\alpha = \cos\alpha, \quad c_\beta = \cos\beta, \quad c_\gamma = \cos\gamma \tag{6}$$

and $R_x(\gamma)$ represents a rotation of γ radians about *x*-axis. Analogously for $R_y(\beta)$ and $R_z(\alpha)$. Moreover, $\alpha, \gamma \in (-\pi, \pi)$ and $\beta \in (-\frac{\pi}{2}, \frac{\pi}{2})$.

SYNCHRONIZATION USING AN ABSOLUTE ORIENTATION SENSOR

In order to make the synchronization of the two platforms it has been used a smart sensor developed by Bosch, the Sensortec BNO055 System in Package (SiP), [7]. It is a 9-axis absolute orientation sensor that integrates a tri-axial 14-bit accelerometer, a tri-axial 16-bit gyroscope with a range of ±2000 degrees per second, a tri-axial geomagnetic sensor and a 32-bit Cortex M0+ microcontroller running Bosch Sensortec sensor fusion software, all in a single package (see Figure 4).

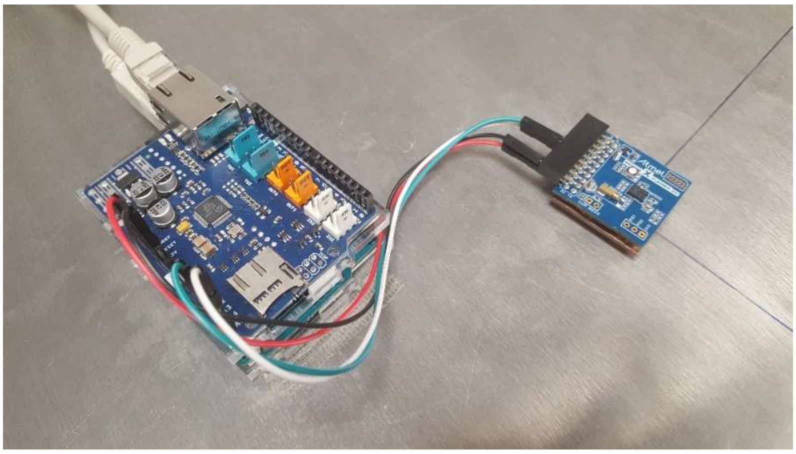

Fig. 4 - Arduino Uno device with Ethernet shield and BNO055 board

Of all of the operation modes that this sensor has, we have chosen the NDOF (Nine Degrees Of Freedom) mode. This is a fusion mode with 9 degrees of freedom where the fused absolute orientation data is calculated from accelerometer, gyroscope and the magnetometer. The advantages of combining all three sensors are a fast calculation, resulting in high output data rate, and high robustness from magnetic field distortions. In this mode the Fast Magnetometer calibration is turned ON and thereby resulting in quick calibration of the magnetometer and higher output data accuracy.

This sensor gives directly the Euler angles at its outputs, but we observed that when the platform tilts these angles becomes increasingly distorted, and sometimes jumps or flips severely. As an alternative, when the quaternion output is selected the data obtained is stable.

We convert the BNO055 quaternion to yaw, pitch and roll angles [8, 9], using the following equations:

$$yaw = atan\left(\frac{2\,(q_X\, q_Y - q_W\, q_Z)}{2\, q_W^2 + 2\, q_X^2 - 1}\right), \tag{7}$$

$$pitch = atan\left(\frac{g_X}{\sqrt{g_Y^2 + g_Z^2}}\right), \tag{8}$$

$$roll = atan\left(\frac{g_Y}{\sqrt{g_X^2 + g_Z^2}}\right), \tag{9}$$

where q_x, q_y, q_z and q_z are quaternion components and g_x, g_y and g_z are gravity vector components computed from quaternion, with

$$g_X = 2\,(q_X\, q_Z - q_W\, q_Y), \tag{10}$$

$$g_Y = 2\,(q_W\, q_X - q_Y\, q_Z), \tag{11}$$

$$g_Z = q_W^2 - q_X^2 - q_Y^2 + q_Z^2 \tag{12}$$

The quaternion is read from the sensor via I2C and using an Arduino Uno it is sent via Ethernet using UDP. UDP (User Datagram Protocol) is an alternative communications protocol to Transmission Control Protocol (TCP) used primarily for establishing low-latency and loss-tolerating connections between applications on the Internet.

Yaw, pitch and roll angles are computed on the platform controller (NI compactRio) since they were originally built on the Arduino, but their math library works with floating point numbers of normal precision and this gives drift problems at the yaw angle. This problem was solved by using double resolution floating-point calculation on the controller [10].

The refresh time of the absolute orientation angles of the platform obtained is 10 ms, the maximum of the sensor, therefore, transmission of data and real-time calculation does not reduce the bandwidth of the sensor.

A problem arises when it is introduced a movement with axes translation. We cannot detect and follow the movement properly because the sensor measures absolute orientation. This problem will be addressed in the near future.

CONCLUSIONS

In this paper, the synchronization in real time of two Stewart platforms, designed and constructed by our research team of the UPC, has been presented. By means of a smart sensor, the synchronization of the platforms has been achieved. The largest platform acts as master while the smaller one acts as slave. The obtained results can be considered very satisfactory since the small platform follows the trajectories with great precision. The details of the synchronization method have been provided.

ACKNOWLEDGMENT

This work has been partially supported by the Spanish Ministry of Economy and Competitiveness under Grant DPI2015-64170-R (MINECO/FEDER).

REFERENCES

[1] Stewart D, A platform with six degrees of freedom, Proceedings of the Institute of Mechanical Engineering, Vol. 180 (5), Part 1, pp.371-386, 1965.

[2] Pedrammehr S, Mahboubkhah M, Khani N, A study on vibration of Stewart platform-based machine tool table, International Journal of Advanced Manufacturing Technology, Vol. 65 (5-8), pp.991-1007, 2013.

[3] Bruzzone L, Molfino R, Razzoli R, Modelling and design of parallel robot for laser cutting applications, Proceedings of the IASTED International Conference on Modelling, Identification and Control, Innsbruck, Austria, February 2002, pp.518-522.

[4] Wapler M, Urban V, Weisener T, Stallkamp J, Durr M, Hiller A, A Stewart platform for precision surgery, Transactions of the Institute of Measurement and Control, Vol. 25 (4), pp.329-334, 2003.

[5] Jáuregui J, Hernández E, Ceccarelli M, López-Cajún C, García A, Kinematic calibration of precise 6-DOF Stewart platform-type positioning systems for radio telescope applications, Frontiers of Mechanical Engineering, Vol. 8 (3), pp.252-260, 2013.

[6] Sam Y, Suib N, Osman J, Proportional integral sliding mode control for the half-car active suspension system with hydraulic actuator, Proceedings of the 8th WSEAS International Conference on Robotics, Control and Manufacturing Technology, Hangzhou, China, April 2008, pp.52-57.

[7] BNO055 data sheet. https://www.bosch-sensortec.com/media/boschsensortec/downloads/smart_sensors_1/bno055/bst-bno055-ds000.pdf

[8] Hazewinkel M, ed. (2001) [1994], Euler angles, Encyclopedia of Mathematics, Springer Science+Business Media B.V./Kluwer Academic Publishers, ISBN 978-1-55608-010-4.

[9] Krey U, Owen A, Basic Theoretical Physics – A Concise Overview, New York, London, Berlin, Heidelberg, Springer, 2007.

[10] Cody WJ *et al.*, IEEE Standards 754 and 854 for Floating-Point Arithmetic. IEEE Magazine MICRO, August 1984, pp.84-100.